Available online at www.sciencedirect.com
SCIENCE DIRECT®
Journal of Organometallic Chemistry 690 (2005) 1324–1331
Journal of Organometallic Chemistry
www.elsevier.com/locate/jorganchem

Cyclic voltammetry and theoretical calculations of silyl-substituted 1,4-benzoquinones

Shinobu Tsutsui [a,*], Kenkichi Sakamoto [a,b,*], Hiroto Yoshida [c], Atsutaka Kunai [c]

[a] *Photodynamics Research Center, RIKEN (The Institute of Physical and Chemical Research), 519-1399 Aoba, Aramaki, Aoba-ku, Sendai 980-0845, Japan*
[b] *Department of Chemistry, Graduate School of Science, Tohoku University, Aoba-ku, Sendai 980-8578, Japan*
[c] *Department of Applied Chemistry, Graduate School of Engineering, Hiroshima University, Higashi-Hiroshima 739-8527, Japan*

Received 10 October 2004; accepted 30 November 2004
Available online 7 February 2005

Abstract

Cyclic voltammograms of 2,3,5,6-tetrakis(trimethylsilyl)-1,4-benzoquinone (**1a**), 2,3,5,6-tetrakis(dimethylvinylsilyl)-1,4-benzoquinone (**1b**), 2,3,5,6-tetrakis(dimethylsilyl)-1,4-benzoquinone (**1c**), 4,4,6,6,10,10,12,12-octamethyl-4,6,10,12-tetrasilatricyclo-[7.3.0.0^{3,7}]dodeca-1(9),3(7)-diene-2,8-dione (**1d**), and 5-*t*-butyl-2-(pentamethyldisilanyl)-1,4-benzoquinone (**5h**) showed that the first reduction step was reversible and that the second step was irreversible. The first half-wave reduction potentials ($E^{I}_{1/2}$s) of **1a**, **1b**, **1c**, and **1d** shifted negatively relative to 1,4-benzoquinone by −0.31, −0.24, −0.03, and −0.18 V, respectively. These results demonstrated that the electron-accepting ability of the chair-form quinones **1a** and **1b** was lower than that of the planar quinones **1c** and **1d**. The $E^{I}_{1/2}$ of **5h** (−0.93 V vs. Ag/Ag^{+}) was quite similar to that of 5-*t*-butyl-2-trimethylsilyl-1,4-benzoquinone (**5a**, −0.94 V). A cyclic voltammogram of dimethylsilylene-bridged 1,4-benzoquinone dimer **7** showed two kinds of $E^{I}_{1/2}$ (−0.76 and −0.94 V). The electrochemical behavior of **7** would be interpreted in terms of near-neighbor interactions between reduced and non-reduced quinone units. Theoretical calculations of the silyl-1,4-benzoquinones reproduced well the solid state structures of the compounds. Also, the computed vibrational frequencies of the silyl-1,4-benzoquinones were in good agreement with the IR absorption frequencies of the C=O units in the compounds. The LUMO energy levels of the silyl-1,4-benzoquinones were quantitatively proportional to the $E^{I}_{1/2}$s.
© 2004 Elsevier B.V. All rights reserved.

Keywords: Organosilicon compound; 1,4-Benzoquinone; Cyclic voltammetry; Theoretical calculations

1. Introduction

1,4-Benzoquinone (quinone) is one of the most important and fundamental π-electron systems because of its high electron affinity and photoreactivity [1]. Although there have been a large number of reports on 1,4-benzoquinone derivatives, very few studies on the silyl-1,4-benzoquinones have been conducted [2–11]. Thus, the chemistry of silyl-substituted 1,4-benzoquinones is of great interest from the viewpoints of the well-known electronic effects and the steric hindrance of the silyl groups towards π-electron systems [12].

1,4-Benzoquinone derivatives usually undergo two-step, one-electron reductions in aprotic solvents to form radical anions and dianions [1]. In 1967, Bock et al. [3a] reported the half-wave reduction potentials ($E^{I}_{1/2}$ and $E^{II}_{1/2}$) of 2,5-bis(trimethylsilyl)-1,4-benzoquinone (**2a**), 2,5-di-*t*-butyl-1,4-benzoquinone (**2g**), and 1,4-benzoquinone (**4**) in acetonitrile with tetra-*n*-butylammonium iodide as the supporting electrolyte against a constant

* Corresponding authors. Tel.: +81 222 282 041; fax: +81 222 282 017.
E-mail addresses: stsutsui@riken.jp (S. Tsutsui), sakamoto@si.chem.tohoku.ac.jp (K. Sakamoto).

0022-328X/$ - see front matter © 2004 Elsevier B.V. All rights reserved.
doi:10.1016/j.jorganchem.2004.11.051

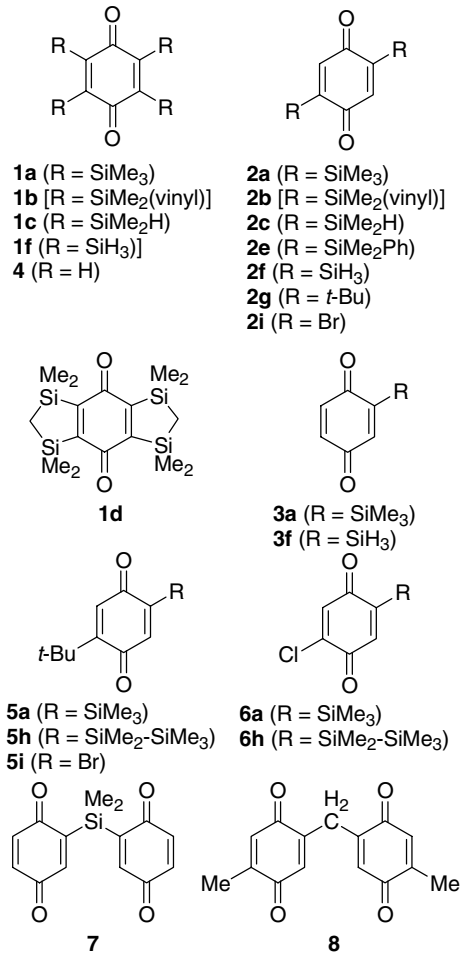

Fig. 1.

mercury anode (Fig. 1). Cyclic voltammograms of the quinones showed two sets of reversible redox peaks. The $E^{I}_{1/2}$s of **2a**, **2g**, and **4** are 0.04, −0.15, and 0.04 V, respectively, and the $E^{II}_{1/2}$s of **2a**, **2g**, and **4** are −0.51, −0.71, and −0.47 V, respectively. The results indicate that the trimethylsilyl and *t*-butyl groups act as electron-donating groups to the 1,4-benzoquinone and the semiquinone radical units.

Very recently, we have reported the $E^{I}_{1/2}$s and $E^{II}_{1/2}$s of 2,3,5,6-tetrakis(trimethylsilyl)-1,4-benzoquinone (**1a**), **2a**, 2-trimethylsilyl-1,4-benzoquinone (**3a**), **4**, and **2g** in acetonitrile with tetra-*n*-butylammonium perchrolate as the supporting electrolyte, referred to an Ag/Ag^{+} redox couple [10]. The $E^{I}_{1/2}$s of **1a**, **2a**, **3a**, and **4**, and **2g** are −1.12, −0.88, −0.85, −0.81, and −1.02 V, respectively. The second reduction step for **1a** is irreversible and the $E^{II}_{1/2}$s of **2a**, **3a**, **4**, and **2g** are −1.55, −1.53, −1.48, −1.74 V, respectively. The $E^{I}_{1/2}$ and $E^{II}_{1/2}$ are observed to have an increasingly negative shift as the number of silyl substituents increased. The results clearly indicate that the silyl group acted as an electron-donating group to the 1,4-benzoquinone and the semiquinone radical units. We explained the stronger electron-accepting ability of **2a** than that of **2g** by the existence of σ*(Si–Me)–π*(quinone) interactions [13] in **2a**.

Recently, we have reported the preparation and structures of **1a**, 2,3,5,6-tetrakis(dimethylvinylsilyl)-1,4-benzoquinone (**1b**), 2,3,5,6-tetrakis(dimethylsilyl)-1,4-benzoquinone (**1c**), and 4,4,6,6,10,10,12,12-octamethyl-4,6,10,12-tetrasilatricyclo[7.3.0.$0^{3,7}$]dodeca-1(9),3(7)-diene-2,8-dione (**1d**) [8,9]. X-ray crystallographic analysis revealed that **1a** and **1b** assume a chair conformation. In contrast to that, **1c** and **1d** have a planar quinone ring. We also reported the preparation and photochemical reaction of 5-*t*-butyl-2-(pentamethyldisilanyl)-1,4-benzoquinone (**5h**) and 5-chloro-2-(pentamethyldisilanyl)-1,4-benzoquinone (**6h**) [6,7]. However, the electrochemical properties of **1b–d**, **5h**, and **6h** have not been successfully analyzed. We report herein the electrochemical properties of a variety of silyl-substituted 1,4-benzoquinones including **1b–d**, **5h**, and **6h** as shown in Fig. 1. The $E^{I}_{1/2}$ of the silicon-bridged 1,4-benzoquinone dimer **7** [11] was also measured. In an effort to elucidate the structures and electronic properties of the silylquinones, density functional theory (DFT) calculations and ab initio molecular orbital (MO) calculations were performed. In particular, the relationship between the LUMO energy levels and the $E_{1/2}$s of the silyl-1,4-benzoquinones will be discussed.

2. Results and discussion

2.1. Cyclic voltammetry

The half-wave reduction potentials ($E^{I}_{1/2}$ and $E^{II}_{1/2}$) of 1,4-benzoquinone derivatives **1–7** were determined by cyclic voltammetry. The $E^{I}_{1/2}$ and $E^{II}_{1/2}$ of **1–7** except for **1d** were measured in an acetonitrile solution containing tetra-*n*-butylammonium perchlorate as the supporting electrolyte, referred to an Ag/Ag^{+} (10 mM) redox couple. Because **1d** was only slightly soluble in acetonitrile, the $E^{I}_{1/2}$ and $E^{II}_{1/2}$ of **1d** were measured in benzonitrile and a 1:1 mixture of acetonitrile/benzonitrile solutions. The $E_{1/2}$ values were determined using the equation, $E_{1/2} = (E_{pa} + E_{pc})/2$, where E_{pa} and E_{pc} represent the anodic and cathodic peak potentials, respectively. Table 1 shows the data obtained from the cyclic voltammograms of 1,4-benzoquinone derivatives. As can be seen in the table, most of the monosilyl- and bissilyl-substituted quinones reveal two sets of reversible redox peaks, which are thought to correspond to 1,4-benzoquinone/semiquinone ($E^{I}_{1/2}$) and semiquinone/hydroquinone dianion ($E^{II}_{1/2}$) couples. The first reduction steps for tetrakissilyl-substituted 1,4-benzoquinones (**1a–d**), 2,5-bis(dimethylsilyl)-substituted 1,4-benzoquinone (**2c**), and pentamethyldisilanyl-substituted 1,4-benzoquinones (**5h** and **6h**) were reversible, while the second

Table 1
Peak potentials of 1,4-benzoquinones in acetonitrile,[a] referred to Ag/Ag^+

Compound	E^I_{pc}	E^I_{pa}	$E^I_{1/2}$	E^{II}_{pc}	E^{II}_{pa}	$E^{II}_{1/2}$
1a	−1.17	−1.06	−1.12 [−0.83]	−1.76	–	Irreversible
1b	−1.10	−0.99	−1.05 [−0.76]	–	–	Irreversible
1c	−0.92	−0.76	−0.84 [−0.55]	−1.61	–	Irreversible
1d[b]	−1.04	−0.94	−0.99 [−0.70]	–	–	Irreversible
1d[c]	(−1.06)	(−0.90)	(−0.98 [−0.69])	–	–	Irreversible
2a	−0.94	−0.82	−0.88 [−0.59]	−1.61	−1.48	−1.55 [−1.26]
2b	−0.88	−0.78	−0.83 [−0.54]	−1.60	−1.50	−1.55 [−1.26]
2c	−0.88	−0.76	−0.82 [−0.53]	Unclear	–	Irreversible
2e	−0.86	−0.76	−0.81 [−0.52]	−1.57	−1.46	−1.52 [−1.23]
2g	−1.07	−0.96	−1.02 [−0.73]	−1.81	−1.66	−1.74 [−1.45]
2i	−0.52	−0.41	−0.47 [−0.18]	−1.21	−1.08	−1.15 [−0.86]
3a	−0.91	−0.78	−0.85 [−0.56]	−1.62	−1.44	−1.53 [−1.24]
4	−0.87	−0.75	−0.81 [−0.52]	−1.56	−1.40	−1.48 [−1.19]
5a	−1.01	−0.87	−0.94 [−0.65]	−1.74	−1.58	−1.66 [−1.37]
5h	−0.98	−0.88	−0.93 [−0.64]	ca.−1.7	–	Irreversible
5i	−0.75	−0.65	−0.70 [−0.41]	−1.54	−1.42	−1.48 [−1.19]
6a	−0.76	−0.63	−0.70 [−0.41]	−1.56	−1.41	−1.49 [−1.20]
6h	−0.70	−0.62	−0.66 [−0.37]	Unclear	–	Irreversible
7	−0.82, −1.00	−0.70, −0.88	−0.76 [−0.47], −0.94 [−0.65]	−1.69	(−1.36)	Irreversible

[a] 1,4-Benzoquinone derivatives: 3 mM, Base solution: acetonitrile supplemented with 100 mM tetra-*n*-butylammonium perchlorate, WE: glassy carbon, RE: $Ag/AgNO_3$ (10 mM) redox couple in base solution, Sweep rate: 100 mV/s. Values in brackets were calibrated to SCE (−0.29 V vs. Ag/Ag^+).
[b] In benzonitrile/acetonitrile = 1:1.
[c] In benzonitrile.

steps were irreversible. This may be due to chemical reactions that occur after the second step.

2.1.1. 2,5-Bissilylquinone series

Because **2a**–**c** and **2e** have a planar quinone ring, the electron-acceptability of **2a**–**c** and **2e** should depend on the electronic effects of the silyl groups. The $E^I_{1/2}$s of **2a**, **2b**, and **2c** shifted negatively relative to that of **4** by −0.07, −0.02, and −0.01 V, respectively, and the $E^I_{1/2}$ of **2e** was equal to that of **4**. The $E^{II}_{1/2}$s of **2a**, **2b**, and **2e** shifted negatively relative to that of **4** by −0.07, −0.07 and −0.04 V, respectively. The results indicate that the silyl groups acted as electron-donating groups to the 1,4-benzoquinone and the semiquinone radical units [10]. The order of the electron-donating ability of the substituents should be *t*-Bu > $SiMe_3$ > $SiMe_2$(vinyl) > $SiMe_2H$ > $SiMe_2Ph$ł > H > Br.

2.1.2. Tetrakissilylquinone series

The $E^I_{1/2}$ of **1d** in a 1:1 mixture of acetonitrile/benzonitrile was −0.99 V, which was quite similar to that measured in benzonitrile (−0.98 V). The $E^I_{1/2}$s of **1a**, **1b**, **1c**, and **1d** shifted negatively relative to that of **4** by −0.31, −0.24, −0.03, and −0.18 V, respectively. The order of the $E^I_{1/2}$s for **1a**, **1b**, **1d**, and **1c** can be understandable by the electron-donating ability of the silyl groups and the deformation of the quinone ring. Both **1a** and **1d** have four trialkylsilyl groups; therefore, the more negative $E^I_{1/2}$ of **1a** than that of **1d** would stem from the deformation of the quinone ring in **1a**. The more negative $E^I_{1/2}$ of **1d** than that of **1c** can be explained by the stronger electron-donating ability of the trialkylsilyl groups than that of the dimethylsilyl groups. The deformation of the ring in **1a** and **1b**, due to the steric repulsion of the pairs of vicinal silyl groups, resulted in the more negative $E^I_{1/2}$s.

2.1.3. Disilanylquinones vs. trimethylsilylquinones

The $E^I_{1/2}$ of 5-*t*-butyl-2-(pentamethyldisilanyl)-1,4-benzoquinone (**5h**) was −0.93 V, which is almost the same as that of 5-*t*-butyl-2-trimethylsilyl-1,4-benozoquinone (**5a**, −0.94 V), while the $E^I_{1/2}$ of 5-chloro-2-(pentamethyldisilanyl)-1,4-benzoquinone (**6h**) was −0.66 V, which is in a region similar to that of 5-chloro-2-trimethylsilyl-1,4-benzoquinone (**6a**, −0.70 V). Judging from the $E^I_{1/2}$s of **5a**, **5h**, **6a**, and **6h**, the electron-donating ability of pentamethyldisilanyl and trimethylsilyl groups to the quinone ring should be almost the same.

2.1.4. Silicon-bridged quinone dimer

Lindsey et al. [14] reported that the half-wave reduction potentials of the methylene-bridged quinone dimer **8** are −0.55, −0.72, and −1.08 V in acetonitrile against a standard calomel electrode. The first and second values are assignable to two kinds of the $E^I_{1/2}$s and the third value is assignable to the $E^{II}_{1/2}$. The authors described that the electrochemical behavior of **8** had been interpreted in terms of near-neighbor interactions between reduced and non-reduced quinone units. Similarly, the $E^I_{1/2}$s of **7** were −0.76 and −0.94 V in acetonitrile referred to

Ag/Ag$^+$. The $E^{II}_{1/2}$ of **7** was not determined due to irreversibility. The difference between the first and second $E^{I}_{1/2}$s of **7** was 0.18 V, which is almost the same as that of **8** (0.17 V) [14].

2.2. Theoretical calculations

To investigate the structures and properties of **1**–**8**, DFT and ab initio MO calculation studies have been conducted [15]. The selected bond lengths and angles (Å and °) for the optimized structure at the B3LYP/6-31G(d) and the solid state structure of **1**–**7** are summarized in Tables 2–5. The vibrational frequencies of the carbonyl units at the B3LYP/6-31G(d) level [16] and the highest occupied molecular orbital (HOMO) and the lowest unoccupied molecular orbital (LUMO) energy levels of **1**–**7** at the MP2/6-311+G(2d,p)//B3LYP/6-31G(d) level are summarized in Table 6. To elucidate the energy and electronic structure of the chair conformation of **1a**, the MO calculations were carried out for **1f-fix**, where the coordinates of the six carbon, two oxygen, and four silicon atoms in **1f** were fixed to those observed for **1a**. Also, the MO calculations were carried out for **4-fix**, where the coordinates of the six carbon and two oxygen atoms in **4** were fixed to those observed for **1a**. The HOMO and LUMO energy levels of **1f-fix** and **4-fix** are listed in Table 6.

2.2.1. Optimized structures and vibrational frequencies

As listed in Tables 2–5, the structural features for the solid state structures of **1**–**7** were fundamentally reproduced by the optimized **1**–**7**. The computed vibrational frequencies of **1**–**7** were in good agreement with the IR absorption frequencies of the C=O units in **1**–**7** (Table 6). While the C–C=C–C torsion angle in the optimized structure of **1c** (10.2°) is slightly larger than that in the solid state structure (3.7°), the calculated vibrational frequency (1625 cm^{-1}) is consistent with the IR absorption frequency of the C=O units (1624 cm^{-1}) [9].

Table 2
Selected average bond lengths and angles (Å and °) for **1a**–**d**

	1a		**1b**		**1c**		**1d**	
	X-ray[a]	DFT[a,b]	X-ray[a]	DFT[b]	X- ray[c]	DFT[b]	X-ray[c]	DFT[b]
Si–C	1.911	1.931	1.911	1.930	1.894	1.919	1.905	1.908
C–C	1.501	1.500	1.497	1.500	1.498	1.496	1.495	1.491
C=C	1.354	1.364	1.360	1.364	1.351	1.362	1.362	1.361
C=O	1.225	1.234	1.227	1.234	1.215	1.235	1.235	1.234
Si–C–C(O)	112.2	112.6	113.1	112.4	112.6	114.0	123.5	123.0
Si–C=C	131.2	131.0	130.2	131.0	128.9	127.7	116.2	116.6
C(O)–C=C	116.6	116.5	116.7	116.6	118.5	118.3	120.4	120.4
C–C(O)–C	123.4	123.8	123.7	123.8	122.7	122.5	119.3	119.2
Si–C=C–Si	17.3	16.9	22.1	18.5	2.8	7.9	0.6	0.0
C–C=C–C	20.0	19.5	18.8	19.1	3.7	10.2	0.5	0.0

[a] Ref. [9].
[b] Calculated at the B3LYP/6-31G(d) level.
[c] Ref. [10].

Table 3
Selected average bond lengths and angles (Å and °) for **2a**–**c** and **2e**

	2a		**2b**		**2c**	**2e**	
	X-ray[a]	DFT[b]	X-ray[c]	DFT[b]	DFT[b]	X-ray[c]	DFT[b]
Si–C	1.873	1.911	1.884	1.911	1.903	1.893	1.912
C–C(Si)	1.487	1.493	1.483	1.494	1.493	1.487	1.494
C=C	1.347	1.351	1.342	1.351	1.351	1.333	1.351
C–C(H)	1.461	1.487	1.468	1.487	1.487	1.482	1.488
C=O	1.233	1.230	1.233	1.230	1.230	1.222	1.230
Si–C–C(O)	119.9	118.8	119.3	118.7	118.7	118.2	118.4
Si–C=C	124.5	123.9	123.6	123.8	123.4	124.4	124.1
C–C(Si)=C	115.6	117.3	117.1	117.5	117.9	117.4	117.5
C(Si)=C–C	123.7	123.6	122.6	123.5	123.1	123.7	123.4
C–C(O)–C	120.8	119.1	120.3	119.0	119.0	118.9	119.1
C–C=C–C	0.5	0.0	1.2	0.9	0.0	3.1	0.0

[a] Ref. [3b].
[b] Calculated at the B3LYP/6-31G(d) level.
[c] Ref. [10].

Table 4
Selected bond lengths and angles (Å and °) for **5** and **6**

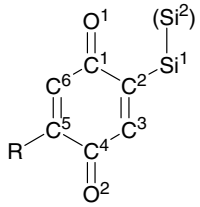

	5a	**5h**	**6a**		**6h**	
	DFT[a]	DFT[a]	X-ray[b]	DFT[a]	X- ray[b]	DFT[a]
Si^1–Si^2	2.374	–	2.349	2.375	–	–
Si^1–C^1	1.912	1.910	1.902	1.916	1.892	1.914
C^1–C^2	1.491	1.492	1.497	1.495	1.494	1.496
C^1–C^6	1.481	1.482	1.480	1.484	1.478	1.485
C^2=C^3	1.350	1.349	1.348	1.351	1.345	1.350
C^3–C^4	1.487	1.489	1.475	1.485	1.479	1.486
C^4–C^5	1.506	1.504	1.487	1.502	1.499	1.501
C^5=C^6	1.351	1.351	1.334	1.343	1.326	1.343
O^1=C^1	1.232	1.230	1.219	1.229	1.224	1.228
O^2=C^4	1.228	1.228	1.223	1.220	1.217	1.219
C^1–C^2–C^3–C^4	0.8	0.0	2.5	0.8	3.0	0.0
C^1–C^6–C^5–C^4	0.4	0.0	3.7	0.4	0.1	0.0
Si^2–Si^1–C^2–C^1	121.2	–	101.5	122.0	–	–
Si^2–Si^1–C^2=C^3	59.7	–	73.7	59.4	–	–

[a] Calculated at the B3LYP/6-31G(d) level.
[b] Ref. [7].

Table 5
Selected average bond lengths and angles (Å and °) for **7**

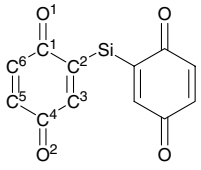

	X-ray[a]	DFT[b]
Si^1–C^1	1.889	1.903
C^1–C^2	1.489	1.494
C^1–C^6	1.481	1.486
C^2=C^3	1.342	1.351
C^3–C^4	1.479	1.487
C^4–C^5	1.470	1.484
C^5=C^6	1.332	1.342
O^1=C^1	1.224	1.229
O^1=C^4	1.227	1.225
C^1–C^2=C^3–C^4	1.5	0.0
C^1–C^6=C^5–C^4	1.0	0.0

[a] Ref. [11].
[b] Calculated at the B3LYP/6-31G(d) level.

2.2.2. HOMO and LUMO energy levels

As can be seen in Fig. 2, the LUMO energy levels were quantitatively proportional to the $E^{I}_{1/2}$s. For example, as the $E^{I}_{1/2}$ of a series of trialkylsilyl-substituted quinones shifts negatively, the corresponding LUMO level increases almost linearly, in the order of **6a** (−0.70 V; −0.16 eV), **3a** (−0.85; −0.09), **2a** (−0.88; 0.20), **5a** (−0.94; 0.27), **1d** (−0.99; 0.33), and **1a** (−1.12; 0.55), proving that the trialkylsilyl group has an electron-donating nature and that the effect is basically cumulative unless other factors would operate.

As for the 2,5-disubstituted quinones, the LUMO energy levels of **2a**–**c**, **2e**–**2g**, and 1,4-benzoquinone (**4**) were estimated to be 0.20, 0.22, 0.09, 0.27, −0.17, 0.35, and −0.03 eV, respectively. The order of the $E^{I}_{1/2}$s for **2g**, **2b**, **2c**, and **4** was consistent with the order expected for the corresponding LUMO energy levels, although little deviation has been seen from the line of the trialkylsilyl series (Fig. 2). The result of the theoretical calculations indicates that the order of the electron-donating ability should be *t*-Bu > $SiMe_2Ph$ > $SiMe_2$(vinyl) = $SiMe_3$ > $SiMe_2H$ > H > SiH_3. However, the higher LUMO level of **2e** (0.27 eV) than that of **2a** (0.20 eV) does not agree with the $E_{1/2}$ of **2e** (−0.81 V) positively shifted relative to that of **2a** (−0.88 V). The reason for the disagreement of the results is unclear. On the other hand, the HOMO energy levels of **2a**, **2b**, **2c**, **2e**, **2f**, **2g**, and **4** were estimated to be −10.56, −10.34, −10.60, −9.27, −11.06, and −10.34 eV, respectively. The order of the HOMOs was not consistent with the order of the corresponding LUMOs and the $E^{I}_{1/2}$s.

For tetra-substituted quinones, the LUMO energy levels of **1a**, **1b**, **1c**, **1d**, **1f**, and **4** were estimated to

Table 6
Peak potentials of 1,4-benzoquinones in acetonitrile, referred to Ag/Ag^+ and summary of energetics of the 1,4-benzoquinone systems

Compound	Calculation			Experiment		
	HOMO[a] (eV)	LUMO[b] (eV)	VF[c,d] (cm^{-1})	CV		IR $\nu_{C=O}$ (cm^{-1})
				$E^{I}_{1/2}$ (V)	$E^{II}_{1/2}$ (V)	
1a	−9.50	0.55	1625	−1.12	Irreversible	1618[e]
1b	−9.50	0.52	1625	−1.05	Irreversible	1624[e]
1c	−9.98	0.15	1625	−0.84	Irreversible	1624[e]
1d	−10.11	0.33	1637	−0.99	Irreversible	1626[e]
1f	−10.89	−0.32	1641	–	–	–
1f-fix	-10.22	0.03	–	–	–	–
2a	−10.56	0.20	1660	−0.88	−1.55	1643[e]
2b	−10.34	0.22	1659	−0.83	−1.55	1643[e]
2c	−10.60	0.09	1661	−0.82	Irreversible	1645[e]
2e	−9.27	0.27	1658	−0.81	−1.52	1645[e]
2f	−11.06	−0.17	1670	–	–	–
2g	−10.34	0.35	1665	−1.02	−1.74	1650
3a	−10.79	0.09	1684, 1664	−0.85	−1.53	1662, 1651[e]
3f	−11.12	−0.11	1687, 1670	–	–	–
4	−11.22	−0.03	1690	−0.81	−1.48	1678, 1658
4-fix	−11.13	0.34	–	–	–	–
5a	−10.45	0.27	1666, 1656	−0.94	−1.66	1651, 1637
5h	−9.64	0.25	1664, 1650	−0.93	Irreversible	1653, 1639[f]
6a	−10.70	−0.16	1698, 1658	−0.70	−1.49	1664, 1637[f]
6h	−9.86	−0.17	1695, 1653	−0.66	Irreversible	1660, 1637[f]
7	−10.80	0.00	1665, 1685	−0.76, −0.94	Irreversible	1656, 1648[g]

[a] Calculated at the B3LYP/6-31(d) level.
[b] Calculated at the MP2/6-311+G(2d,p) level.
[c] Vibrational frequency.
[d] Multipled by a scale factor of 0.9614.
[e] Ref. [9].
[f] Ref. [7].
[g] Ref. [11].

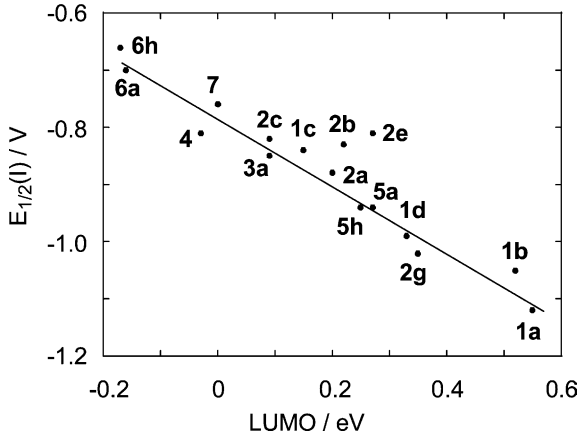

Fig. 2. A plot of the LUMO energy levels vs. the $E^{I}_{1/2}$s of **1**–**7**. There is a linear correlation for **1a**, **1d**, **2a**, **3a**, **5a**, and **6a** ($R = 0.9952$).

be 0.55, 0.52, 0.15, 0.33, −0.32, and −0.03 eV, respectively. The order of the $E^{I}_{1/2}$s for **1a**, **1b**, **1d**, **1c**, and **4** was again consistent with the order expected for the corresponding LUMO energy levels. While the HOMO and LUMO energy levels of **1f-fix** are 0.67 and 0.35 eV higher than those of **1f**, respectively, those of **4-fix** are 0.09 and 0.37 eV higher than those of **4**, respectively (Table 6). The results indicated that the higher-lying HOMOs of **1a** and **1b** are not caused by the deformation of the quinone rings but the introduction of the silyl groups. On the other hand, the higher-lying LUMOs of **1a** and **1b** would stem from the deformation of the quinone ring.

The LUMO energy levels of **5h** and **6h** (0.25 and −0.17 eV) are similar to those of **5a** and **6a** (0.27 and −0.16 eV). The result was consistent with the similarity of the $E_{1/2}$s of **5h** and **6h** (−0.93 and −0.66 V) to those of **5a** and **6a** (−0.94 and −0.70 V). This means that the electron-donating abilities of trimethylsilyl and pentamethyldisilanyl groups to the LUMO energy levels of **5** and **6** are almost the same. In contrast to that, the HOMO energy level of **5h** (−9.64 eV) is 0.81 eV higher than that of **5a** (−10.45 eV). Similarly, the HOMO energy level of **6h** (−9.86 eV) is 0.84 eV higher than that of **6a** (−10.70 eV). The higher HOMO levels of **5h** and **6h** would be explained by the σ(Si–Si)–π(quinone) interaction [6,7]. The σ−π interaction should be effective at the HOMO energy level and ineffective at the LUMO energy level.

While the LUMO and (LUMO + 1) energy levels of **7** are 0.00 and 0.02 eV, respectively, the LUMO and (LUMO + 1) energy levels of **8** are 0.02 and 0.17 eV,

respectively. The nearly degenerated LUMO and (LUMO + 1) energy levels of **7** and **8** suggested that the interactions between the two quinone units are weak in the LUMOs of **7** and **8**. The differences between the first and second $E^{I}_{1/2}$s of **7** (0.18 V) and **8** (0.17 V) would stem from the near-neighbor interactions between reduced and non-reduced quinone units in **7** and **8**. In other words, the Coulomb repulsion between the semiquinone radicals and the neutral quinones would play a major role in the electronic properties of **7** and **8**.

In summary, the HOMOs and the LUMOs shifted to higher energies as the number of silyl groups increased, whereas the calculated vibrational frequencies shifted to lower frequencies. The result of the calculations also indicates that the silyl groups acted as electron-donating substituents. The LUMO energy levels of **1**–**7** were quantitatively proportional to the $E^{I}_{1/2}$s of **1**–**7**.

3. Conclusion

The cyclic voltammograms of 2,3,5,6-tetrakis(trimethylsilyl)-1,4-benzoquinone (**1a**), 2,3,5,6-tetrakis(dimethylvinylsilyl)-1,4-benzoquinone (**1b**), 2,3,5,6-tetrakis (dimethylsilyl)-1,4-benzoquinone (**1c**), 4,4,6,6,10,10,12,12-octamethyl-4,6,10,12-tetrasilatricyclo[7.3.0.0^{3,7}]dodeca-1(9),3(7)-diene-2,8-dione (**1d**), 2,5-bis(dimethylsilyl)-1,4-benzoquinone (**2c**), 5-*t*-butyl-2-(pentamethyldisilanyl)-1,4-benzoquinone (**5h**), and 5-chloro-2-(pentamethyldisilanyl)-1,4-benzoquinone (**6h**) showed that the first reduction step was reversible and that the second reduction step was irreversible. The first half-wave reduction potentials ($E^{I}_{1/2}$s) of **1a**, **1b**, **1c**, and **1d** shifted negatively relative to 1,4-benzoquinone (**4**) by −0.31, −0.24, −0.03, and −0.18 V, respectively. These results demonstrated that the electron-accepting ability of the chair-form quinones **1a** and **1b** was lower than that of the planar quinones **1c** and **1d**. The $E^{I}_{1/2}$ of **5h** (−0.93 V) was quite similar to that of 5-*t*-butyl-2-trimethylsilyl-1,4-benzoquinone (**5a**, −0.94 V). The cyclic voltammogram of dimethylsilylene-bridged 1,4-benzoquinone dimer **7** showed two kinds of $E^{I}_{1/2}$ which were −0.76 and −0.94 V, which means that the Coulomb repulsion between reduced and non-reduced quinone units exist. Theoretical calculations for silyl-substituted 1,4-benzoquinones indicated that the LUMOs shifted to higher energies, whereas the calculated vibrational frequencies shifted to lower frequencies as the number of silyl groups increased. The theoretical calculation of the silylquinones reproduced well the solid state structures, the IR absorption frequencies of the carbonyl units, and the first half-wave reduction potentials of the compounds.

4. Experimental

4.1. General methods

^{1}H, ^{13}C, and ^{29}Si NMR spectra were recorded on a Varian INOVA 300 FT-NMR spectrometer at 300, 75.4, and 59.6 MHz, respectively. Mass spectra were recorded on Shimadzu GCMS-QP5050A and HITACHI M-2500 mass spectrometers. IR spectra were recorded on a HORIBA FT-710 Fourier transform infrared spectrometer. Gel permeation chromatography (GPC) was conducted on a LC908-C60 recycling high-pressure liquid chromatograph (Japan Analytical Instruments Co., Ltd.) using JAIGEL-1H (40 mm × 600 mm), JAIGEL-2H (40 mm × 600 mm), and JAIGEL-2.5H (40 mm × 600 mm) columns, using chloroform as an eluent.

4.2. Materials

2,3,5,6-Tetrakis(trimethylsilyl)-1,4-benzoquinone (**1a**) [9], 2,3,5,6-tetrakis(dimethylvinylsilyl)-1,4-benzoquinone (**1b**) [9], 2,3,5,6-tetrakis(dimethylsilyl)-1,4-benzoquinone (**1c**) [9], 4,4,6,6,10,10,12,12-octamethyl-4,6,10,12-tetrasilatricyclo[7.3.0.0^{3,7}]dodeca-1(9),3(7)-diene-2,8-dione (**1d**) [9], 2,5-bis(dimethylvinylsilyl)-1,4-benzoquinone (**2b**) [9], 2,5-bis(dimethylsilyl)-1,4-benzoquinone (**2c**) [9], 2,5-bis(dimethylphenylsilyl)-1,4-benzoquinone (**2e**) [9], 2,5-dibromo-1,4-benzoquinone (**2i**) [17], 2-trimethylsilyl-1,4-benzoquinone (**3a**) [9], 5-*t*-butyl-2-(pentamethyldisilanyl)-1,4-benzoquinone (**5h**) [7], 5-chloro-2-trimethylsilyl-1,4-benzoquinone (**6a**) [7], 5-chloro-2-(pentamethyldisilanyl)-1,4-benzoquinone (**6h**) [7], and silicon-bridged quinone dimer **7** [11] were prepared according to the procedures previously reported. 2,5-Bis(trimethylsilyl)-1,4-benzoquinone (**2a**) [3], and (4-*t*-butyl-2,5-dimethoxyphenyl)trimethylsilane were prepared as described in the Supplementary material. Cerium ammonium nitrate (CAN), acetonitrile, chloroform, hexane, sodium chloride, anhydrous magnesium sulfate, toluene, and $CDCl_3$ were obtained from standard commercial sources.

4.3. Preparation of 5-t-butyl-2-trimethylsilyl-1,4-benzoquinone (*5a*)

A mixture of (4-*t*-butyl-2,5-dimethoxyphenyl)trimethylsilane (345 mg, 1.30 mmol), CAN (2.34 g, 4.27 mmol), acetonitrile (120 mL), and water (80 mL) was stirred at room temperature for 17 h. The mixture was hydrolyzed with water. The organic layer was separated and the aqueous layer was extracted with hexane. The organic layer and the extracts were combined, washed with water and brine, dried over anhydrous magnesium sulfate, and filtered. The filtrate was concentrated under reduced pressure, and the residue was chromatographed on silica gel using toluene as the eluent to give 5-*t*-butyl-

2-trimethylsilyl-1,4-benzoquinone (**5a**, 168 mg, 0.710 mmol, 55%). **5a**: orange crystals; m.p. 157.0–158.3 °C; ^{1}H NMR ($CDCl_3$, δ) 0.21 (s, 9H), 1.25 (s, 9H), 6.54 (s, 1H), 6.74 (s, 1H); ^{13}C NMR ($CDCl_3$, δ) −1.78, 29.02, 34.98, 132.78, 145.57, 149.99, 155.60, 187.07, 191.81; ^{29}Si NMR ($CDCl_3$, δ) −4.18; IR (neat) $\nu_{C=O}$ 1651, 1637 cm^{-1}; MS (70 eV) *m/z* (%) 236 (M^+, 37), 221 (100), 193 (69); Anal. Found: C, 65.95; H, 8.54%. Calc. for $C_{13}H_{20}O_2Si$: C, 66.05; H, 8.53%.

4.4. Cyclic voltammetric measurements

Voltammetric measurements were conducted with 3 mM of 1,4-benzoquinones in a base solution under a nitrogen atmosphere. The base solution was acetonitrile containing 100 mM of tetra-*n*-butylammonium perchlorate as the supporting electrolyte. Because **1d** was only slightly soluble in acetonitrile, the voltammetric measurements of **1d** were measured in benzonitrile and a 1:1 mixture of acetonitrile/benzonitrile solutions. The peak potentials listed in Tables 1 and 6 were determined at a sweep rate of 100 mV/s using an $Ag/AgNO_3$ (10 mM) reference electrode. A glassy carbon disk (diameter; 5 mm) with a Teflon cap was used as the working electrode, and the surface of the disk was polished using alumina powders and washed with acetonitrile prior to each measurement. The $E_{1/2}$ values were determined as $(E_{pa} + E_{pc})/2$, where E_{pa} and E_{pc} represent the anodic and cathodic peak potentials, respectively.

4.5. Theoretical calculations

All geometry optimization and subsequent vibrational frequency calculations were performed at the B3LYP/6-31G(d) level. These were followed by single-point calculations at the MP2/6-311+G(2d,p) level. The theoretical calculations were performed using the GAUSSIAN 03 program [15]. The computed frequencies were multiplied by a scale factor of 0.9614 in order to correct for the anharmonicity of the vibrations [16].

Acknowledgement

We thank Dr. Hiromasa Tanaka (RIKEN) for fruitful discussions on the theoretical calculations.

Appendix A. Supplementary data

Supplementary data associated with this article can be found, in the online version, at doi:10.1016/j.jorganchem.2004.11.051.

References

[1] For reviews on quinones. See: (a) R.H. Thomson, in: S. Patai, Z. Rappoport (Eds.), The Chemistry of the Quinonoid Compounds, John Wiley & Sons, Bristol, 1974;
(b) Y. Naruta, K. Maruyama, in: S. Patai, Z. Rappoport (Eds.), The Chemistry of the Quinonoid Compounds, vol. 2, John Wiley & Sons, New York, 1988.
[2] (a) G.D. Cooper, B. Williams, C.P. Lape, J. Org. Chem. 26 (1961) 4171;
(b) H. Hashimoto, Yakugaku Zasshi 87 (1967) 535.
[3] (a) H. Bock, H. Alt, Angew. Chem., Int. Ed. Engl. 6 (1967) 941;
(b) H. Bock, S. Nick, C. Nather, K. Ruppert, Z. Naturforsch., Teil B 50 (1995) 595.
[4] (a) N.S. Vasileiskaya, L.V. Gorbunova, O.N. Mamysheva, G.N. Bortnikov, Izv. Akad. Nauk. SSSR Ser. Khim. (1972) 2755;
(b) L.D. Foland, J.O. Karlsson, S.T. Perri, R. Schwabe, S.L. Xu, S. Patil, H.W. Moore, J. Am. Chem. Soc. 111 (1989) 975.
[5] S. Tsutsui, K. Sakamoto, Chem. Commun. (2003) 2322.
[6] (a) K. Sakamoto, H. Sakurai, J. Am. Chem. Soc. 113 (1991) 1466;
(b) H. Sakurai, J. Abe, K. Sakamoto, J. Photochem. Photobiol. A 65 (1992) 111.
[7] S. Tsutsui, K. Sakamoto, K. Ebata, C. Kabuto, H. Sakurai, Bull. Chem. Soc. Jpn. 75 (2002) 2661.
[8] S. Tsutsui, K. Sakamoto, K. Ebata, C. Kabuto, H. Sakurai, Chem. Lett. (2000) 226.
[9] S. Tsutsui, K. Sakamoto, K. Ebata, C. Kabuto, H. Sakurai, Bull. Chem. Soc. Jpn. 75 (2002) 2571.
[10] S. Tsutsui, K. Sakamoto, H. Yoshida, A. Kunai, Organometallics 23 (2004) 1554.
[11] S. Tsutsui, H. Tanaka, K. Sakamoto, Organometallics 23 (2004) 3719.
[12] For reviews on silyl-substituted π-electron systems. See: (a) H. Sakurai, Nippon Kagaku Kaishi (1990) 439;
(b) H. Sakurai, Pure Appl. Chem. 68 (1996) 327;
(c) T. Matsuo, A. Sekiguchi, Bull. Chem. Soc. Jpn. 77 (2004) 211.
[13] (a) Y. Apeloig, in: S. Patai, Z. Rappoport (Eds.), The Chemistry of Organic Silicon Compounds, Part 1, John Wiley, New York, 1989 (Chapter 2 and references therein);
(b) C.G. Pitt, J. Organomet. Chem. 61 (1973) 49;
(c) C.G. Pitt, J. Organomet. Chem. 23 (1970) C35;
(d) P.v.R. Schleyer, T. Clark, A.J. Kos, G.W. Spitznagel, C. Rohde, D. Arad, K.N. Houk, N.G. Rondan, J. Am. Chem. Soc. 106 (1984) 6467;
(e) W. Setaka, C. Kabuto, M. Kira, Chem. Lett. (1999) 317.
[14] A.S. Lindsey, M.E. Peover, N.G. Savill, J. Chem. Soc. (1962) 4558.
[15] M.J. Frisch, G.W.S.H.B. Trucks, G.E. Scuseria, M.A. Robb, J.R. Cheeseman, J.A. Montgomery Jr., T. Vreven, K.N. Kudin, J.C. Burant, J.C. Millam, S.S. Iyengar, J. Tomasi, V. Barone, B. Mennucci, M. Cossi, G. Scalmani, N. Rega, G.A. Petersson, H. Nakatsuji, M. Hada, M. Ehara, K. Toyota, R. Fukuda, J. Hasegawa, M. Ishida, T. Nakajima, Y. Honda, O. Kitao, H. Nakai, M. Klene, X. Li, J.E. Knox, H.P. Hratchian, J.B. Cross, C. Adamo, J. Jaramillo, R. Gomperts, R.E. Stratmann, O. Yazyev, A.J. Austin, R. Cammi, C. Pomelli, J.W. Ochterski, P.Y. Ayala, K. Morokuma, G.A. Voth, P. Salvador, J.J. Dannenberg, V.G. Zakrzewski, S. Dapprich, A.D. Daniels, M.C. Strain, O. Farkas, D.K. Malick, A.D. Rabuck, K. Raghavachari, J.B. Foresman, J.V. Ortiz, Q. Cui, A.G. Baboul, S. Clifford, J. Cioslowski, B.B. Stefanov, G. Liu, A. Liashenko, P. Piskorz, I. Komaromi, R.L. Martin, D.J. Fox, T. Keith, M.A. Al-Laham, C.Y. Peng, A. Nanayakkara, M. Challacombe, P.M.W. Gill, B. Johnson, W. Chen, M.W. Wong, C. Gonzalez, J.A. Pople, GAUSSIAN 03, Revision B.03, Gaussian Inc., Pittsburgh PA, 2003.
[16] A.P. Scott, L. Radom, J. Phys. Chem. 100 (1996) 16502.
[17] J.F. Bagli, Ph. L'Ecuyer, Can. J. Chem. 39 (1961) 1037.